ELSEVIER

PII: S0141-0296(97)00079-5

Engineering Structures, Vol. 20, No. 3, pp. 144–154, 1998

0141-0296/98 $19.00 + 0.00

Implementation issues and testing of a hybrid sliding isolation system

M. A. Riley and A. M. Reinhorn

Department of Civil Engineering, State University of New York at Buffalo, Buffalo, NY 14260, USA

S. Nagarajaiah

Department of Civil Engineering, University of Missouri-Columbia, Columbia, MO 65211, USA

Structural control systems can effectively protect structures from dynamic loads. Passive control systems are widely accepted, but active and hybrid systems remain under development with a variety of implementation related issues yet to be resolved. The current research focuses on overcoming some of these problems. A hybrid sliding isolation system is considered. This nonlinear controller is ideal for examining many practical issues; moreover, results obtained with this system may be applied to a variety of active and hybrid controllers. New nonlinear control algorithms, which account for implementation imperfections, are developed and validated with realistic experimental models. The results show that the control system is able to significantly reduce the peak responses and the energy input, proving that many of the implementation issues may be overcome with well designed controllers and current technology. © 1997 Published by Elsevier Science Ltd.

Keywords: active control, hybrid systems, nonlinear control, sliding systems, implementation, experimentation, shaking table, seismic excitations

1. Introduction

Dynamic environmental loads, such as earthquakes and strong winds, can seriously damage, or even destroy, bridges and bulidings. The strengthening of structures to withstand extreme dynamic loads can be uneconomical or impractical; moreover, constructing a conventional building with the strength to withstand large seismic motion may lead to a situation where the structure is undamaged, but the structure's contents are damaged or destroyed, and the structure's occupants injured. The need to economically protect structures, their occupants and their contents has led to the development of innovative protective systems, which either isolate structures from the dynamic load, or dissipate the destructive energy that enters the structure. These structural control systems can be classified into three categories: passive systems, active systems and hybrid systems.

Typical passive control devices include mass dampers, which control the structural resonse through energy transfer from the main structure to the moving mass, structural dampers, which dissipate energy, and base isolation systems, which decouple the motion of the structure from the seismic vibrations. Active systems use an intelligent controller to sense either the excitation, the structural response, or both, and introduce control forces through special actuators or devices. The devices, which include active mass dampers and active tendon systems, require a relatively large supply of power to generate the active forces.

Hybrid control systems combine active controllers with passive devices. In most hybrid control systems, such as hybrid isolation systems, hybrid mass dampers and semi-active structural dampers, the active portion of the system is used to influence the response of the passive control device, minimizing the structural response. The active portion of a hybrid system requires much less power than a similar active system, while providing better structural response than the passive system alone. In addition, hybrid systems tend to have better fail-safe characteristics than the active systems.

Unfortunately, there are a variety of problems and limitations associated with the implementation of structural control systems. The effectiveness of passive controllers

tends to be limited by the system design, while active systems may require a large amount of power, have questionable reliability, and require a high level of maintenance. Hybrid systems may be more expensive than active or passive systems, require the same maintenance as active ones, but they have the reliability of the passive system.

There are additional problems related to the practical implementation of control algorithms for both active and hybrid systems. These problems, which include signal noise, modeling errors, actuator–structure interaction, delays, and other uncertainties, can increase the difficulty of developing a controller and can limit its effectiveness. An additional problem, system nonlinearities, complicates the development of control algorithms for hybrid and active systems.

2. Integral problems in structural control

In an ideal situation, a simple active controller can be designed based on linear control theory, with disregard for the many problems and imperfections that are present in a typical system. Unfortunately, such a controller will be likely to perform poorly, if it is implemented in a realistic structural system. The problems and limitations that can affect a structural control system need to be considered in the design of the system. These issues can be loosely grouped into two classes: (i) physically solvable, and (ii) computationally solvable. The problems that can be classified as physically solvable tend to be related to the long term viability and reliability of the control system, while the problems that are computationally solvable tend to be related to the response of the controller and the interaction between the controller and structural system.

The effectiveness of any control system can be maximized by optimizing the design; however, there are limitations to the effectiveness of each control system. Passive systems tend to be limited by physical constraints, while active and hybrid systems tend to be limited by the capability of the control algorithms, energy requirements, and cost.

Some of the computationally solvable issues that must be considered in the design of a control algorithm for active and hybrid systems include: the stability of the control, the effects of delays, the noise in the digitized instrumentation signals, the dynamics of any filters required to attenuate the signal noise, the interaction between the actuator and structure, the potential for actuator saturation, any system nonlinearities, the limits of system identification, and errors in the system mode, including any unmodeled modes of vibration.

The stability of a linear system, without signal noise or unmodelled dynamics, can usually be easily proven. The stability of nonlinear systems may be more difficult to prove, but methods based on the work of Lyapunov are usually sufficient[1,2]. Unfortunately, in the presence of a number of uncertainties, such as typically found in a practical control system, there is a potential for unanticipated instabilities if the uncertainties are not accounted for.

The effects of delays can be critical to the performance of the control system. Digital computers can cause a significant delay in the feedback loop, due to the time required for digitizing analog signals, performing the control calculation, and converting the digital control signal back to an analog signal. In addition, unmodeled dynamics in filters, instruments, and actuators, will cause time lags, which will degrade the performance of the system, unless they are accounted for.

The noise in the instrumentation signals will adversely affect the control response, and the nature of analog circuitry guarantees that there will be some noise in any analog signal. This noise, as well as high frequency responses in the instrument and higher mode response in the structure, can appear as an aliased low frequency response when the analog signal is digitized, unless a low pass filter is used to attenuate the noise. Frequency components of the noise that fall within the bandwidth of the controller cannot be removed from the signals. To protect the system from the adverse effects of this noise, care must be taken to keep the signal to noise ratio high, and the controller must be sufficiently robust, so as to remain stable in the presence of such uncertainty.

The filters that are used to remoe the high frequency components of the noise from the instrumentation signals have their own dynamic characteristics. Typical low pass analog filters, such as used for antialiasing purposes, have a unit response amplitude over the passband, and then roll off exponentially above it. The filters will also introduce a phase lag in the filtered signal. When the type and order of the filters are known, the dynamics of the filters can be easily modeled, and the phase lag accurately accounted for.

The devices used to provide the control forces are themselves dynamic systems. As an actuator applies forces to the structural system, the structure is in turn applying forces on the actuator, exciting the actuator's dynamics. Recent research[3,4] has shown the importance of properly modeling the dynamics of the actuator and accounting for the interaction between the structure and the actuator. An additional problem is encountered when actuator saturation occurs. In the presence of saturation, the actuator dynamics, which otherwise may be linear, will become nonlinear. The case of actuator saturation can be modeled and accounted for in the control, or the system can be designed such that actuator saturation is avoided.

The greatest single source of error may be the analytical model of the structure. Although most laboratory models are carefully designed to have a nearly linear response, realistic structural systems tend to have some nonlinear response, and in some cases may be highly nonlinear. Due to limitations in modeling and system identification theory, the exact identification of structural parameters is virtually impossible; however, for most systems the parameters may be estimated with a reasonable level of accuracy. For a typical implementation of structural control, a continuous and nonlinear structure must be modeled as a system with a discrete number of modes of vibration; moreover, the structure will usually be modeled as a linear system, unless the nonlinearities are large. The control algorithm that is developed for this system will have errors, even if the limitations and uncertainties described above were not present. This is not to say that such a structural model is entirely flawed. If the structure model is carefully chosen, significant nonlinearities are accounted for, and the system parameters are properly identified, then the error in the analytical model should be minimal and tolerable for most situations.

3. Hybrid isolation systems

Hybrid isolation systems have recently received attention as a way of improving the performance of passive base

isolation systems. The considerable amount of research performed on passive isolation systems, and the growing body of data collected from constructed base isolated structures, shows that properly designed passive isolation systems are extremely effective for reducing the energy input to a structure; unfortunately, there are well defined, physical limitations to the efficiency of these systems. Hybrid systems present a way to further improve the response of isolation systems, using an active controller to modify and improve the response of a passive isolation system.

Friction controlled, sliding hybrid isolation systems, which are the primary focus of the current study, using sliding bearings to isolate a structural system, and add an actuator, connected between the foundation and the basemat of the structure, to provide active control forces[5]. A few types of sliding bearings have been proposed for use in these systems, including ball or roller bearings, and conventional Teflon–steel sliding bearings[3,6]. In both cases, the control forces can be designed to offset the friction forces in the bearings, control the basement displacement, minimize certain structural responses, or perform a combination of these functions. Ideally, the control force could simply offset the friction forces, creating a 'frictionless' isolation system, however, imperfections in the system lead to undesired responses[7].

Hybrid systems incorporating Teflon–steel bearings have been extensively modeled and experimentally tested. Analytical research has considered the use of hybrid sliding isolation in both single- and multi-degree-of-freedom systems, such as bridges[8], rigid structures on a sliding basemat[9,10], and three and eight story structures[11]. A significant amount of experimental research has been performed, including studies on a scale system designed to model a bridge[3,8] or rigid structure[6], a 1/4 scale, three-story structure[3,5,7,12], and an isolated floor system designed to protect secondary system[13]. This research has shown that the hybrid control reduces the response of the isolated system[3,6,8,14]. The presented research will show that unless the affects of the imperfections ae considered in the control design, the control system cannot be implemented.

4. Integral algorithms for hybrid systems

A wide variety of control algorithms have been proposed for controlling hybrid systems, and research is constantly in progress to find additional efficient and improved control algorithms. Hybrid systems do not necessarily require different control algorithms than active systems, but the nonlinear nature of many hybrid systems has lead to the consideration of increasingly sophisticated algorithms. A comparison of some linear and nonlinear control algorithms has shown that the nonlinear algorithms provide better response in one controlled system[14]. The nonlinear control algorithms that have been considered include control laws based on instantaneous optimal control, dynamic linearization, fuzzy control, sliding mode control, adaptive control and pulse control. Some of these algorithms have been experimentally tested, while others have only been analytically or numerically verified.

4.1. Modeling of the nonlinear hybrid system

The control algorithms used for nonlinear hybrid systems must be closely integrated with the model of the structural systems. For the case of the hybrid system on sliding bearings, a conventional structural model can be used for the superstructure, but the nonlinearity of the isolation system will need special treatment. The structural system will be modeled as a multi-degree-of-freedom shear frame structure mounted on a rigid sliding basemat. Including the friction forces in the sliding isolation and the control force from the hybrid controller, the equation of motion is:

$$\mathbf{M}\ddot{\mathbf{x}}_t + \mathbf{C}\dot{\mathbf{x}} + \mathbf{K}\mathbf{x} + \mathbf{D}\mathbf{f}_f = \mathbf{D}\mathbf{u} \tag{1}$$

Here, **M**, **C** and **K** are the mass damping, and stiffness matrices, $\mathbf{f}_f$ and **u** are the nonlinear friction force and control force vectors, **D** defines the locations and directions of the forces, while **x** and $\mathbf{x}_t$ are the relative and absolute displacement vectors. For the equations of motion to be consistent, all of the elements in the direction vector, **D**, must be either zero or one, each column must have exactly one non-zero element, no row can have more than one non-zero element, and $\mathbf{D}^T\mathbf{D} = \mathbf{I}$. The relationship between the absolute and the relative displacements is given by:

$$\mathbf{x}_t = \mathbf{x} + \mathbf{R}\mathbf{x}_g \tag{2}$$

Here, $\mathbf{x}_g$ is the ground displacement vector, and **R** defines which component of the ground motion is associated with each degree-of-freedom. Since many controls laws are more easily developed using a state space formulation, the state vector can be defined as:

$$\mathbf{z} = \begin{Bmatrix} \mathbf{x} \\ \dot{\mathbf{x}} \end{Bmatrix} \tag{3}$$

The equation of motion can then be reformulated into state space, as:

$$\dot{\mathbf{z}} = \mathbf{A}\mathbf{z} + \mathbf{B}\mathbf{u} - \mathbf{B}\mathbf{f}_f - \mathbf{W}\ddot{\mathbf{x}}_g \tag{4}$$

Here, **A** is the system state matrix, while **B** and **W** are the external force location and ground acceleration direction vectors. These are defined as:

$$\mathbf{A} = \begin{bmatrix} 0 & \mathbf{I} \\ -\mathbf{M}^{-1}\mathbf{K} & -M^{-1}\mathbf{C} \end{bmatrix}; \mathbf{B} = \begin{bmatrix} 0 \\ \mathbf{M}^{-1}\mathbf{D} \end{bmatrix}; \mathbf{W} = \begin{bmatrix} 0 \\ \mathbf{R} \end{bmatrix} \tag{5}$$

The most general model for the friction forces at a sliding interface can be defined as:

$$f_f = \mu mgy \tag{6}$$

Here f_f is the friction force, μ is the coefficient of friction, m is the total mass, g is the gravitational acceleration, and y is a dimensionless hysteretic parameter that defines the direction of the friction force and the stick slip conditions. For a system with Teflon–steel bearings, the friction coefficient can be modeled as[15]:

$$\mu = \mu_{\max} - \mu_\Delta e^{-\mu_a|\dot{x}|} \tag{7}$$

Where $\dot{x}$ is the relative velocity at the sliding interface, $\mu_{\max}$ is the coefficient of friction at high velocities, μ_Δ is the change in the coefficient, and μ_a defines the rate of variation. The hysteretic parameter can be defined by either a differential equation[3,10,15] or by a simple Coulomb model.

To control this hybrid isolation system, control algor-

ithms based on the instantaneous optimal control law, fuzzy set theory, and dynamic linearization were developed. These control algorithms are reported in detail in other sources[3,6–8,10], but an overview is included here.

4.2. Absolute acceleration control

The absolute acceleration control algorithm[6,8] is based on the instantaneous optimal control law, developed by Yang[11]. This control algorithm uses acceleration feedback to attempt to minimize the response of the hybrid system. Two versions of the algorithm were developed and tested: the linear absolute acceleration control and the nonlinear absolute acceleration control.

The absolute acceleration control is formulated in state space, with the motion of the system given by equation (4). Based on the instantaneous optimal control law, the control force can be found by minimizing a time dependent performance index[11], given as:

$$J(t) = \dot{\mathbf{z}}^{\mathrm{T}}\mathbf{Q}\dot{\mathbf{z}} + \mathbf{u}^{\mathrm{T}}\mathbf{R}\mathbf{u} \tag{8}$$

Here $J(t)$ is the instantaneous optimal performance index, while $\mathbf{Q}$ and $\mathbf{R}$ are positive semidefinite weighting matrices for the response and control force, respectively.

Minimization of the performance index to determine the control force can be achieved by a procedure developed by Yang[16], and the control force can be determined to be[8,16]:

$$\mathbf{u} = -\mathbf{R}^{-1}\mathbf{B}^{\mathrm{T}}\mathbf{Q}\dot{\mathbf{z}} \tag{9}$$

The response of the controlled system is dependent on the choice of the weighting matrices, $\mathbf{Q}$ and $\mathbf{R}$. Since, the control force is a product of these matrices, one weighting matrix can always be identity. For the case of absolute acceleration control, the control force weighting matrix, $\mathbf{R}$, was set to identity, and the state weighting matrix, $\mathbf{Q}$, was adjusted to define the control force. For the case of the linear absolute acceleration control, $\mathbf{Q}$ is a diagonal matrix with constant gain terms that multiply the acceleration[6,8].

The nonlinear absolute acceleration control is an expansion of the linear control algorithm. The control gain is now chosen so that it varies as an exponential function of the absolute acceleration. The control force weighting matrix will again be a diagonal matrix with the individual terms defined as[5]:

$$q_{i,i} = \alpha_i[1 - e^{-\beta_i|\ddot{x}_i|}] \tag{10}$$

Here $q_{i,i}$ is the ith diagonal term in the control force weighting matrix, while α_i and β_i are the associated gain factors. The first gain factor, α_i, will be similar to the gain factor for the linear control algorithm, while the second gain factor, β_i, will vary based on signal noise levels and actuator limitations. This control algorithm will respond with an increased gain as the magnitude of the acceleration increases, while responding with a low gain for small accelerations, minimizing the effects of noise in the signal.

4.2.1. Fuzzy sets control Controllers based on fuzzy set theory form a simple way to specify nonlinear control laws that are capable of accommodating a high level of uncertainty and imprecision. These fuzzy controllers can be used in two conditions. When linguistic descriptions of the control can be formulated, a fuzzy controller may be determined without a mathematical model[7,10], but if no linguistic description is available, one may be implemented using a fuzzy mathematical model of the system. Two fuzzy control algorithms were developed for the hybrid isolation system[7,10]. For an ideal system, given by equation (1), the control force may be designed to exactly oppose the reaction forces in the isolation, and the control force will be:

$$\mathbf{u} = \mathbf{D}^{\mathrm{T}}\mathbf{C}\dot{\mathbf{x}} + \mathbf{D}^{\mathrm{T}}\mathbf{K}\mathbf{x} + \mathbf{f}_{\mathrm{f}} \tag{11}$$

This implies that the total absolute acceleration of the controlled system will always be zero.

In any realistic system, the errors and uncertainties will significantly degrade the effectiveness of the controller. The relative displacement and velocity measurements will contaminated by sensor noise, limitations in system identification techniques will reduce the accuracy of the damping and stiffness coefficients, while the effects of delay and actuator dynamics will degrade the accuracy of the control force. The combination of these problems will lead to an inaccurate control force that is based on an estimate of the forces at the time of interest.

Using the symbol * to indicate that a term is an estimate of the real value, with some associated error, the estimated control force can be defined as:

$$\mathbf{u} = \mathbf{D}^{\mathrm{T}}\mathbf{C}^*\dot{\mathbf{x}}^* + \mathbf{D}^{\mathrm{T}}\mathbf{K}^*\mathbf{x}^* + \mathbf{f}_{\mathrm{f}}^* \tag{12}$$

This results in an imperfect control, and the absolute acceleration will not vanish. Instead:

$$\mathbf{M}(\ddot{\mathbf{x}}+\mathbf{R}\ddot{\mathbf{x}}_{\mathrm{g}}) = \mathbf{M}\boldsymbol{\epsilon}_{\mathrm{t}} \tag{13}$$

Here $\boldsymbol{\epsilon}_{\mathrm{t}}$ is a vector of the deviations in the absolute accelerations, which acts as a measure of the error in the control force. Accurate modeling of this error is difficult by conventional techniques, making compensation quite complicated, however fuzzy logic provides a simple way to deal with this error, by compensating for the imprecision and uncertainty[7,10].

Two formulations of the fuzzy control have been developed for the hybrid system: the total force formulation and the increment force formulation. In the total force formulation, the control force is determined by approximating the forces in the system and measuring the absolute acceleration that remains. When the relative velocities and displacements are large, the estimates of the forces are usually good, and the control force may be accurately estimated. However, when the relative velocities are small, a slight error in the estimate of the relative velocity may cause a significant error in estimate of the friction, and the control will be inefficient. In the latter case, a direct measurement of the difference in the forces and the absolute acceleration is necessary to determine the change in the control force from one time step to the next. This second method is defined as the incremental force formulation[10].

The fuzzy controller generates a precise control force by using an inference scheme to quantify imprecise fuzzy sets. The controller has three main components, as shown in *Figure 1*. In the fuzzification step, the response of the system is converted from digital values to quantities expressed in terms of fuzzy sets. Through fuzzy processing, the fuzzy response data is manipulated by a series of linguistic rules to produce a series of control force fuzzy sets. By defuzz-

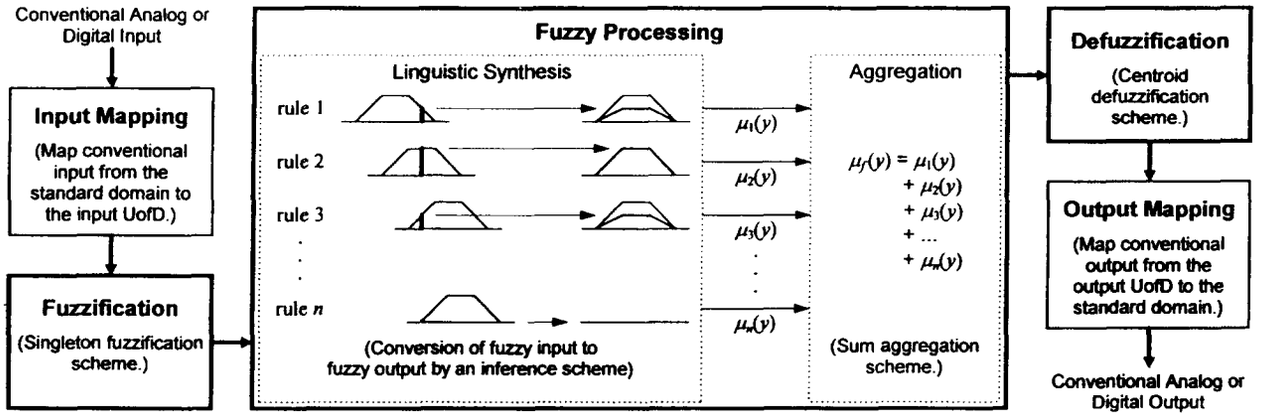

Figure 1 Schematic of a fuzzy controller

ification, these sets are converted into a precise control force that can be applied to the hybrid system[7].

The fuzzy controller handles system nonlinearities and uncertainties in a flexible manner. Noise and delays can be compensated in the fuzzification and processing stages of the fuzzy algorithm, while the processing stage can be used to explicitly consider structural nonlinearities. Actuator errors and limitations can be considered in defuzzification and processing stages.

The fuzzy controller has several other advantages over conventional controllers[10]. It can be designed to discriminate between inputs of varying importance, treating each according to its importance. The output aggregation and defuzzification schemes can reduce the affects of noise and computer imprecision, and when trapezoidal shaped fuzzy sets are used, the input signals are implicitly filtered. The way in which the fuzzy sets account for noise and uncertainty can be understood by examining the plot of input and output fuzzy sets, shown in *Figure 2*. Each fuzzy set is named with a linguistic term, with the ZE fuzzy set corresponding to values of zero and nearly zero. Since small errors can cause instability in the control when the input is small, the ZE set encompasses a range of small input values where control may not be desirable. By allowing this region of no action, the fuzzy controller can stabilize the control when the inputs are small.

4.2.2. Friction force control The nonlinear nature of the sliding interface creates a need for a control algorithm that can explicitly account for the variations in the friction force. The method of dynamic linearization, is used to develop the friction force control algorithm, which explicitly accounts for the nonlinearity in the sliding isolation, and implicitly minimizes the effects of delays, signal noise, actuator dynamics, and filter dynamics. Details of the technique can be found in a number of sources[1,3,17,18]. Two variations of the friction force control algorithm were developed and experimentally tested. The relative displacement formulation is based on the actual dynamics of the hybrid isolation system, and controls both the effective force at the friction interface and the relative position of the structure. The absolute displacement formulation is based on the dynamics of a structure that is connected by a spring to a fixed inertial reference. This second formulation controls both the effective force and absolute position of the structure.

For the method of dynamic linearization, a linear template system is chosen and the control force necessary to create this system is determined. The most ideal system has no lateral motion, and its absolute accelerations, velocities, and displacements will be zero at all times. Comparing on this template system to the system described in equation (1), the ideal control force will be:

$$\mathbf{u} = \mathbf{D}^{\mathrm{T}}\mathbf{C}\dot{\mathbf{x}} + \mathbf{D}^{\mathrm{T}}\mathbf{K}\mathbf{x} + \mathbf{f}_{\mathrm{f}} \tag{14}$$

Unfortunately, the actual control force will vary from the desired control force due to the errors and uncertainties in the system. Using the symbol * to indicate that a term is

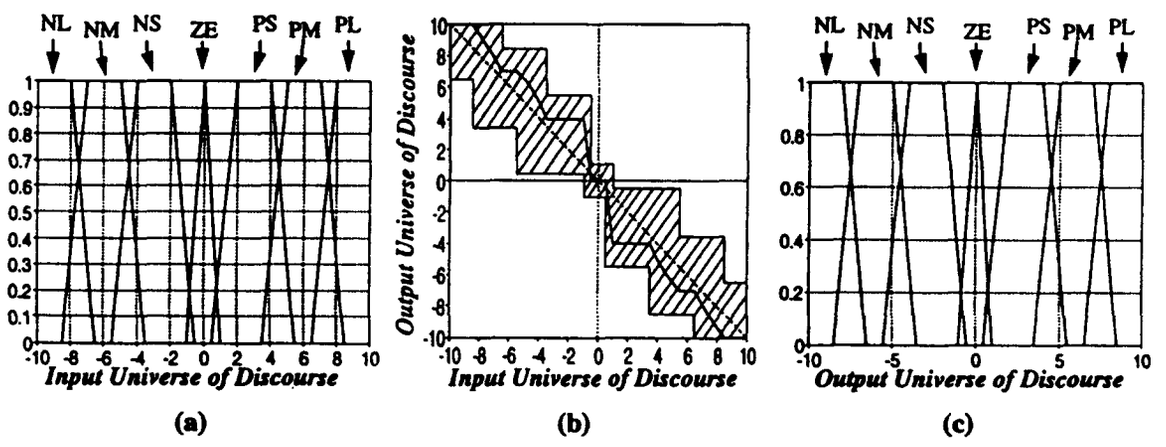

Figure 2 Input and output fuzzy set distributions

an imperfect estimation of the actual value, the actual control force may be described by:

$$\mathbf{u} = \mathbf{D}^T\mathbf{C}^*\dot{\mathbf{x}}^* + \mathbf{D}^T\mathbf{K}^*\mathbf{x}^* + \mathbf{f}_f \tag{15}$$

The products of the estimated terms in the control force can be redefined as:

$$\mathbf{C}^*\dot{\mathbf{x}}^* = \mathbf{e}_c\mathbf{C}\dot{\mathbf{x}};\ \mathbf{K}^*\mathbf{x}^* = \mathbf{e}_k\mathbf{K}\mathbf{x};\ \mathbf{f}_f^* = \mathbf{e}_f\mathbf{f}_f \tag{16}$$

where $\mathbf{e}_c$, $\mathbf{e}_k$, and $\mathbf{e}_f$ are diagonal matrices of error terms describing the ratio between the true forces in the system and the estimated forces. The equation of motion is then:

$$\mathbf{M}\ddot{\mathbf{x}}_t + (\mathbf{I}-\mathbf{e}_c)\mathbf{C}\dot{\mathbf{x}} + (\mathbf{I}-\mathbf{e}_k)\mathbf{K}\mathbf{x} + (\mathbf{I}-\mathbf{e}_f)\mathbf{D}\mathbf{f}_f = \mathbf{0} \tag{17}$$

When the terms in the error matrices all approach one, the system will behave in the ideal manner, and when the terms of the error matrices are small the system will behave in an uncontrolled manner. Most importantly, when the terms in the error matrices are greater than one or negative, the controller will drive the system instead of controlling it. To prevent this last case from occurring, the components of the control force can be multiplied by a series of gain factors, G_c, G_k and G_f. The control force becomes:

$$\mathbf{u} = G_c\mathbf{D}^T\mathbf{e}_c\mathbf{C}\dot{\mathbf{x}} + G_k\mathbf{D}^T\mathbf{e}_k\mathbf{K}\mathbf{x} + G_f\mathbf{e}_f\mathbf{f}_f \tag{18}$$

For stable control, the gain factors must be chosen so that the terms $G_c\mathbf{e}_c$, $G_k\mathbf{e}_k$, and $G_f\mathbf{e}_f$ are always less than one[3]. Since the error terms may be greater than one, the gain factors must always be less than one, moreover, the products of the gain factors and the error matrices will usually be somewhat smaller than one, and some acceleration will occur in the system.

To minimize the acceleration of the controlled system, the acceleration term can be considered in the control algorithm. The acceleration term will have an error, $\mathbf{e}_I$, associated with it, and require a gain factor, G_I. Like the other gain factors, the acceleration gain is bounded based on the stability requirements, but because the noise and delays tend to have a greater effect on the acceleration term, the acceleration gain should usually be small. Adding the acceleration term to the control force leads to:

$$\mathbf{u} = G_c\mathbf{D}^T\mathbf{e}_c\mathbf{C}\dot{\mathbf{x}} + G_k\mathbf{D}^T\mathbf{e}_k\mathbf{K}\mathbf{x} + G_f\mathbf{e}_f\mathbf{f}_f - G_I\mathbf{D}^T\mathbf{e}_I\mathbf{M}\ddot{\mathbf{x}}_t \tag{19}$$

To further improve the response of the controlled system, the effects of the noise in the response signals and the delays in the system need to be considered. The noise should generally be small as compared to the average magnitude of the signal. Thus, when the magnitude of a response signal is large, the affect of the noise on the control signal will be small, however, when the signal is small, the noise may be of the same order of magnitude or greater than the actual signal. In a similar way, when the phase shift caused by the delay is small, the error due to the delay will be negligible when the response is large, but the error may be much larger than the actual signal when the response becomes small. A new error term can be defined for each signal, based on the expected peak magnitude of the combined noise and delay errors. These individual error terms may be combined into a series of error vectors, $\boldsymbol{\epsilon}_x$, $\boldsymbol{\epsilon}_{\dot{x}}$, and $\boldsymbol{\epsilon}_{\ddot{x}_t}$. Noting that the error in the control will become large as the magnitude of a signal approaches the associated error term, the control force can be redefined as a discontinuous function that does not control a particular term when the magnitude of the response signal for that term is below a threshold level. Using the error vectors as the threshold levels, the control force can be defined as:

$$\begin{aligned}\mathbf{u} = {} & G_c\mathbf{D}^T\mathbf{e}_c\mathbf{C}\dot{\mathbf{x}}[\upsilon(|\dot{\mathbf{x}}|-\boldsymbol{\epsilon}_{\dot{x}})] + G_k\mathbf{D}^T\mathbf{e}_k\mathbf{K}\mathbf{x}[\upsilon(|\mathbf{x}|-\boldsymbol{\epsilon}_x)] \\ & G_f\mathbf{e}_f\mathbf{f}_f[\upsilon(|\dot{\mathbf{x}}|-\boldsymbol{\epsilon}_{\dot{x}})] - G_I\mathbf{D}^T\mathbf{e}_I\mathbf{M}\ddot{\mathbf{x}}[\upsilon(|\ddot{\mathbf{x}}_t|-\boldsymbol{\epsilon}_{\ddot{x}_t})]\end{aligned} \tag{20}$$

where $\upsilon()$ is the unit step function. This formulation is the relative displacement friction force control.

A second variation of the friction force control algorithm is the absolute displacement friction force control. Since the relative formulation does not consider the absolute position of the structure, there is a tendency for the system to drift away from the initial position. The absolute formulation is based on minimizing the absolute position of the system instead of the absolute acceleration. This version is developed in much the same way as the relative formulation, but a different template system is used. The template system for the absolute formulation is defined as:

$$\mathbf{M}\ddot{\mathbf{x}}_t + K_v\mathbf{x}_t = 0 \tag{21}$$

Here K_v is the virtual stiffness of an imaginary spring attached between the structural system and an absolute inertial reference. Combining the linear template system with the equation of motion given in equation (1) yields an ideal control force:

$$\mathbf{u} = \mathbf{D}^T\mathbf{C}\dot{\mathbf{x}} + \mathbf{D}^T\mathbf{K}\mathbf{x} - K_v\mathbf{D}^T\mathbf{x}_t + \mathbf{f}_f \tag{22}$$

The same problems that complicate the relative formulation will apply to this formulation, so the appropriate gain factors and error thresholds must be added. Since the virtual stiffness is only defined in the control force, there is no need for a gain factor for this term. Including all necessary gains and error thresholds, the absolute displacement formulation control force is:

$$\begin{aligned}\mathbf{u} = {} & G_c\mathbf{D}^T\mathbf{e}_c\mathbf{C}\dot{\mathbf{x}}[\upsilon(|\dot{\mathbf{x}}|-\boldsymbol{\epsilon}_{\dot{x}})] + G_k\mathbf{D}^T\mathbf{e}_k\mathbf{K}\mathbf{x}[\upsilon(|\mathbf{x}|-\epsilon_x)] \\ & - K_v\mathbf{D}^T\mathbf{e}_v\mathbf{x}_t[\upsilon(|\mathbf{x}_t|-\boldsymbol{\epsilon}_{x_t})] + G_f\mathbf{e}_f\mathbf{f}_f[\upsilon|\dot{\mathbf{x}}|-\boldsymbol{\epsilon}_{\dot{x}})] \\ & - G_I\mathbf{D}^T\mathbf{e}_I\mathbf{M}\ddot{\mathbf{x}}_t[\upsilon(|\ddot{\mathbf{x}}_t|-\boldsymbol{\epsilon}_{\ddot{x}_t})]\end{aligned} \tag{23}$$

where $\boldsymbol{\epsilon}_v$ and $\boldsymbol{\epsilon}_{x_t}$ are the error matrix and error magnitude vector associated with the absolute displacement. The stability of these two control algorithms can be proven explicitly by a combination of the method of Lyapunov[1] and the invariant set theorem[2]. The results of the stability analysis will define the limits for each of the gain factors. Details of these results can be found elsewhere[3].

5. Model hybrid isolation system

To verify the proposed control algorithms, an experimental model of the hybrid isolation system was constructed. The experimental model was tested in a variety structural configurations, including a three-degree-of-freedom building on base isolation. Experimental tests were conducted with the base of the structure fixed, to model a conventional

structure, with the base of the structure free to slide, to model a passive isolation system, and with the base motion controlled by the hybrid isolation system. The sliding isolation was designed to realistically model an efficient structural isolation system, so a meaningful comparison can be made between the responses of the hybrid and passive sliding systems.

The rigid structural basemat, shown in *Figure 3*, was designed to accommodate a variety of model structural systems and to allow control devices to be mounted beneath it. The mounting surface was constructed from a 1630 mm (64 in) by 1020 mm (40 in) by 50.8 mm (2 in) thick steel plate. The plate was stiffened lengthwise with four L 4×4×4×3/4″ steel angles. Two W 12×35 beams were used as legs, to create enough clear height beneath the mounting plate for installation of the controller and springs. Each of the beams were stiffened with six welded diaphragms, made from 25.4 mm (1 in) thick steel plate. The resulting basemat weighed 10.4 kN (2330 lb), and was sufficiently stiff, so as to be considered rigid in the current tests.

The basemat was mounted on four sliding bearings, consisting of high strength woven Teflon pads riding on mirror finish stainless steel plates. The stainless steel plates were mounted steel foundations, which were precisely leveled and grouted in place, while the Teflon pads were mounted on the botton of the basemat with leveling plates that were adjusted so that the equal loads were carried by each of the bearings. The contact area of each of the Teflon pads was 31.7 mm^2 (0.049 in^2), for a total contact area of 126.8 mm^2 (0.196 in^2).

The friction forces in the bearings were modeled using the relationship described in equations (6) and (7). The coefficient of friction at high velocities, μ_{max}, was found to be 0.06, and the change in the coefficient of friction, μ_Δ, was found to be 0.03. The rate of change of the coefficient of friction, μ_a, was determined to be 0.09 s/mm (2.29 s/in).

Two helical steel springs were used to provide restoring forces. These springs were mounted on either side of the basemat, and provided forces through shear deformation. The springs had a combined stiffness of 0.072 kN/mm (410 lb/in), which gave the system a reasonable period for an isolated structure.

A three-story, steel frame model was mounted on the basemat. The one-quarter scale model structure, shown in *Figure 4*, has been used extensively in previous control experiments at the University of Buffalo[19]. This model is 2540 mm (100 in) high and 610 mm (24 in) by 1220 mm (48 in) in plan. The first story of the structure is 1020 mm (40 in) high, and the upper two stories have heights of 760 mm (30 in). All of the experimental tests were performed with the direction of the ground motion parallel to the long direction of the structure. To minimize out of plane motions, the structure was stiffened with diagonal bracing in the weak direction.

The steel frame of the structure weighs 2.31 kN (520 lb), and rigid steel masses, each weighing 8.68 kN (1950 lb) are bolted to each floor of the structure. The total weight of the structure and the three masses was 28.35 kN (6370 lb). For testing and analysis purposes, the structure was assumed to behave as a lumped mass model, with the weight of the structural frame distributed to the three rigid

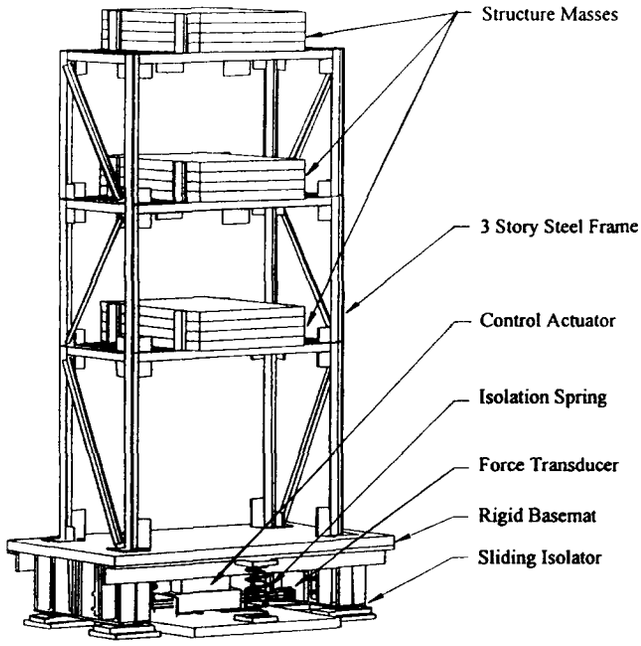

Figure 4 Three story structural model on sliding basemat

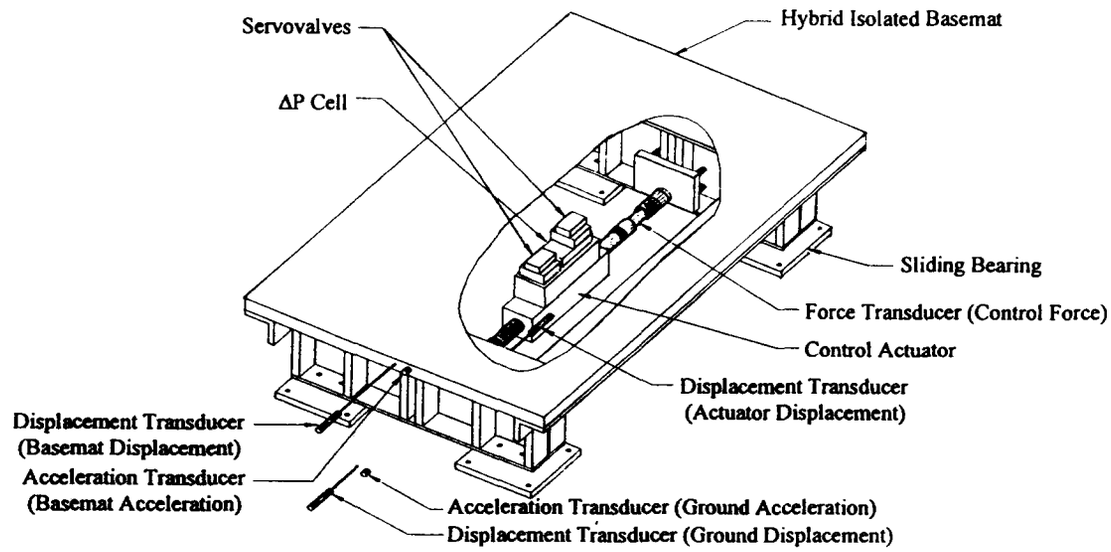

Figure 3 Sketch of rigid basemat on sliding isolation

masses. In this configuration, the superstructure had primary natural frequencies of 1.95, 6.7 and 12.3 Hz, with damping ratios of 0.49, 0.44 and 0.40%. The combined isolated system had natural frequencies of 0.65, 3.32, 7.40 and 12.85 Hz, with damping ratios of 1.25, 0.43, 0.45 and 0.41%. The mass, damping, stiffness, and mode shape matrices for the system are given in *Table 1*.

The control forces were provided by a 24.5 kN (5500 lb) double-rod servo-hydraulic actuator with a piston cross section of 1200 mm^2 (1.9 in^2) and a dynamic stroke of 152 mm (6 in). During the control tests the stroke was electronically limited to 127 mm (5.0 in) to prevent accidental over-travel, although the actuator had built-in hydraulic buffers to prevent the actuator from being damaged if the stroke limits were reached. Two 0.95 l/s (15 gal/min), two stage servovalves were used in parallel to provide up to 1.90 l/s (30 gal/min) of hydraulic fluid to the cylinder, allowing the actuator to provide velocities of up to 1580 mm/s (62 in/s).

A set of coupled force transducers, or load cells, were used as the primary control sensors. These strain gage based sensors, were constructed from stainless steel cylinders and designed to have a linear range of ±55.6 kN (±12,500 lb). The transducers were constructed with resistive foil strain gages arrayed in a full Wheatstone bridge such that bending and thermal strains would be automatically canceled, and only the axial strains would be measured. Since both ends of the actuator rod were applying forces at the same time, the two transducers were wired together with one transducer reporting a positive load in compression, while the other transducer reported a negative load in comparison. The combined transducers were then calibrated as single a unit for an axial load range of ±44.50 kN (±10,000 lb) about a preload point of 26.70 kN (6000 lb) of compression. This combined sensor had an accuracy of approximately ±0.089 kN (±20.0 lb) at full scale.

The actuator's servovalve was driven by a dedicated analog servocontroller, with the control signal generated by a digital microcomputer. To protect the model structure from damage if the control system failed to perform properly, an analog fail-safe circuit, which was capable of shutting down the control hydraulics, was used to monitor the response of the system. A custom software program was written implement the algorithms used to control the hybrid isolation system. The experimental tests were performed at the National Center for Earthquake Engineering Research Structural Engineering Laboratory at the University at Buffalo. The current experiments utilized a variety of equipment, including the seismic simulator, a number of transducers for monitoring the structural response, signal conditioners, and a high speed data acquisition system.

The experimental program consisted of a number of identification tests, folllowed by tests of the structural controllers, each with a variety of ground motions. The ground motions consisted of a banded white noise excitation, and a number of scaled earthquake records, including the S00E component of the El Centro record from the 1940 Imperial Valley earthquake, the N21E component of the Taft record from the 1952 Kern County earthquake, the North–South component of the Hachinohe record from the 1968 Tokachi-Oki earthquake, and the S16E component of the Pacoima Dam record from the 1971 San Fernando earthquake.

Table 1 Structural property matrices for hybrid isolated structure

Property	Matrix
Mass (kg)	$\begin{bmatrix} 963 & 0 & 0 & 0 \\ 0 & 963 & 0 & 0 \\ 0 & 0 & 963 & 0 \\ 0 & 0 & 0 & 1060 \end{bmatrix}$
Stiffness (kN/mm)	$\begin{bmatrix} 1.256 & -1.612 & 0.587 & -0.230 \\ -1.612 & 3.012 & -2.076 & 0.667 \\ 0.587 & -2.076 & 3.245 & -1.756 \\ -0.230 & 0.667 & -1.756 & 1.391 \end{bmatrix}$
Damping (kN s/mm)	$\begin{bmatrix} 254.9 & -165.5 & 9.8 & -3.3 \\ -165.6 & 393.6 & -149.2 & 16.3 \\ 9.8 & -149.2 & 410.8 & -173.5 \\ -3.3 & 16.3 & -173.5 & 278.0 \end{bmatrix} \times 10^{-6}$
Modal shapes	$\begin{bmatrix} 1.000 & 1.000 & 1.000 & 1.000 \\ 0.980 & 0.486 & -0.977 & -2.146 \\ 0.921 & -0.506 & -0.943 & 2.257 \\ 0.869 & -1.055 & 0.863 & -1.020 \end{bmatrix}$

6. Results of experimental tests

Tests were performed with the hybrid isolated three-story structural model controlled by four different algorithms: the relative and absolute formulations of the friction force control, linear absolute acceleration control, and fuzzy sets control. All four algorithms tended to reduce the peak structural responses as compared to the fixed base and passive isolated systems. The relative formulation of the friction force control produced the best overall response in the peak story accelerations, listed in *Table 2*, while the absolute formulation performed nearly as well. Both of these algorithms tended to reduce the peak accelerations to about half of the passive response and to less than 25% of the fixed base response. Neither the linear absolute acceleration control nor the fuzzy sets control reduced the accelerations as well, but both performed better than the passive isolation.

Control of the interstory drifts and base shear forces is important to prevent damage to the structure. As listed in *Table 2*, all four control algorithms reduced the peak drifts and base shears significantly more than the passive isolation system. The two formulations of the friction force control performed similarly, and produced the smallest drifts, while the absolute acceleration control reduced the base shears the most. The fuzzy sets control produced the smallest reductions, but still improved the response as compared to the passive isolation.

The difference in the responses of the passive and hybrid system are due in part to the way the isolation reacts to various levels of excitation. The passive isolation tended to slide only during the most intense ground motion, which kept the base displacements reasonable, but limited the improvements in the structural response. The hybrid isolation caused the system to slide at lower levels of excitation and to remain sliding for a longer period. The resulting basemat displacements were generally larger than those in the passive case, however, the structural response was reduced more.

The improvements in the structural response came at the expense of significant control resources. The drift in the basemat and the required control forces are both important when judging the hybrid control. The control forces and basemat displacements can be considered to be the control resources, while reducing the story accelerations, interstory

Table 2 Comparison of the peak structural responses

Earthquake (1)	Nominal PGA (g) (2)	Base fixed (3)	Passive isolation (4)	Response of three-story structure Relative FFC (5)	Absolute FFC (6)	Linear AAC (7)	Fuzzy sets control (8)
				Peak story acceleration (g)			
El Centro	0.34	1.19	0.46	0.20	0.19	0.23	0.22
Hachinohe	0.23	0.93	0.32	0.16	0.18	0.24	0.29
Pacoima	0.40	1.57	0.32	0.15	0.16	0.32	0.27
Taft	0.32	1.20	0.39	0.19	0.20	0.30	0.31
White noise 0–20 Hz	0.20	0.85	0.34	0.17	0.22	0.29	0.28
				Peak story drift			
El Centro	0.34	22.0	5.5	3.6	3.6	4.8	4.7
Hachinohe	0.23	23.6	5.6	3.6	3.1	3.9	4.8
Pacoima	0.40	29.0	4.8	2.7	3.0	4.0	4.4
Taft	0.32	24.1	6.1	4.0	3.4	3.8	5.8
White noise 0–20 Hz	0.20	19.1	4.6	2.9	3.0	3.3	4.8
				Base shear coefficient			
El Centro	0.34	0.57	0.15	0.10	0.10	0.08	0.13
Hachinohe	0.23	0.61	0.15	0.08	0.08	0.10	0.14
Pacoima	0.40	0.77	0.13	0.08	0.09	0.07	0.11
Taft	0.32	0.64	0.12	0.10	0.10	0.09	0.13
White noise 0–20 Hz	0.20	0.48	0.14	0.08	0.09	0.08	0.11

drifts, and base shears can be considered to be the control objective. The fuzzy sets control was not highly effective at controlling the objectives, but required the fewest resources. The linear absolute acceleration control was quite effective for two of the three objectives, but required fewer control resources than the friction force control. The relative formulation of the friction force control met the control objectives quite well, but produced very large base displacements. The absolute formulation was developed as a solution to this problem, and was able to limit the peak basemat displacements to the same range as the fuzzy sets and absolute acceleration controls. Unfortunately, both formulations of the friction force control required greater control forces than the other algorithms.

6.1. *Energy response*

The peak and RMS responses provide only a partial picture of how an excitation is influencing the structural system. In many cases, the energy in the system is a better gauge of how the structure is being affected. A single spike in the acceleration response may not significantly affect the structural system, but give the appearance that the response is relatively poor. Similarly, a single cycle of motion with large interstory drifts may cause less damage than a large number of cycles of motion with smaller drifts. In cases such as these, the energy that must be dissipated by the structure is a better gauge of how the system is responding.

The energy response of the hybrid isolated structure was developed using the methods described by Uang and Bertero[20]. A thorough development and discussion of the energy response of the isolated system can be found elsewhere[3]. The energy response of the fixed base, passive isolated, and hybrid systems controlled with the friction force control were compared to determine the influence that the control had on the amount of energy the structures were required to dissipate.

The passive isolation significantly reduced the amount of viscous damping energy that had to be dissipated, as listed in *Table 3*, while the hybrid isolation systems reduced this energy even further. The relative formulation of the friction force control reduced the dissipated energy by 76–96% as compared to the fixed base structure, and as compared to the passive isolation, by 2–36% during all tests except the Hachinohe earthquake record. The absolute formulation performed even better, reducing the peak dissipated energies by 83–99% as compared to the fixed base structure, and 35–89% as compared to the passive isolated structure.

The input energy is most important, since it is the total energy that enters superstructure and will have to be released or dissipated. By itself, the passive isolation reduced the input energies by 71–92%. The relative formulation of the friction force control further reduced the input energy by 78–93% as compared to the fixed base structure, and 10–71% as compared to the passive isolated structure. The absolute formulation performed slightly better, producing reductions of 84–96% as compared to the conventional structure, and 39–55% as compared to the passive isolated structure.

The energies dissipated in the sliding isolation and the control energies tended to be large in comparison to the structural energies. The hybrid controllers caused the energy dissipated in the sliding isolation to increase of 1.7–3.2 times. These large increases are due to the large control energies used by the hybrid system. As listed in *Table 3*, both formulations of the friction force control used control energies that were much greater than the reductions in the structural energy, making the controllers quite inefficient. The relative formulation had energy efficiencies of just 0.3–9.3%, while the absolute formulation had efficiencies of 2.1–5.5%.

The apparent efficiencies of the hybrid controllers are reduced by considering the effect of the control on the superstructure alone. A significant portion of the control energy is expended to reduce the response of the structure's basemat. When the input energy to the entire structural system is considered, the efficiencies increase dramatically, to a range of 21–49%.

Table 3 Comparison of the energy response in the three-story model structure

Earthquake (1)	Nominal PGA (g) (2)	Peak response: Base fixed (3)	Peak response: Passive isolation (4)	Peak response: Relative FFC (5)	Peak response: Absolute FFC (6)	Response ratios: Passive/ base fixed (7)	Response ratios: Rel. FFC/ base fixed (8)	Response ratios: Abs. FFC/ base fixed (9)	Response ratios: Rel. FFC/ passive (10)	Response ratios: Abs. FFC/ passive (11)
					Viscous damping energy (J)					
El Centro	0.34	150.1	28.7	26.6	10.9	0.19	0.18	0.07	0.93	0.38
Hachinohe	0.23	329.1	7.0	18.8	1.3	0.02	0.06	0.00	2.68	0.19
Pacoima	0.40	121.7	11.0	4.8	1.2	0.09	0.04	0.01	0.44	0.11
Taft	0.32	175.2	46.7	42.6	30.3	0.27	0.24	0.17	0.91	0.65
White noise 0–20 Hz	0.20	286.1	35.6	34.8	22.5	0.12	0.12	0.08	0.98	0.63
					Excitation input energy (J)					
El Centro	0.34	176.5	51.4	32.1	28.7	0.29	0.18	0.16	0.62	0.56
Hachinohe	0.230.40	385.0	29.7	26.9	16.8	0.08	0.07	0.04	0.90	0.56
Pacoima	0.32	143.9	37.4	10.7	17.0	0.26	0.07	0.12	0.29	0.45
Taft	0.20	230.5	67.4	51.1	37.8	0.29	0.22	0.16	0.76	0.56
White noise 0–20 Hz		395.5	67.6	45.0	41.1	0.17	0.11	0.10	0.67	0.61
					Control energy (J)					
El Centro	0.340.23	—	—	813	560	—	—	—	—	—
Hachinohe	0.40	—	—	822	615	—	—	—	—	—
Pacoima	0.32	—	—	286	371	—	—	—	—	—
Taft	0.20	—	—	872	1010	—	—	—	—	—
White noise 0–20 Hz		—	—	1539	1155	—	—	—	—	—

This poor efficiency of the hybrid controlled system was partially due to the physical imperfections of the system, which limited the effectiveness of the control. To some extent, the friction force controllers were able to overcome these imperfections by implicitly accounting for the control errors that these imperfections cause, however, the effectiveness of the controllers remained somewhat limited. Still, both of the formulations of the friction force control performed well. The absolute formulation as somewhat more efficient than the relative formulation, producing equivalent results without significantly increasing the basemat displacements beyond the levels in the passive isolation.

7. Concluding remarks

Specialized control algorithms, which account for the sources of error and uncertainty in the controlled system, have been developed for controlling nonlinear hybrid systems. By accounting for the nonlinearities, physical limitations, and imperfections in the hybrid system, these controllers can remain stable and effective in realistic implementations.

The current experimental results reaffirm previous work that has shown sliding isolation systems to significantly reduce the response of structural systems during earthquakes. More importantly, these experimental results prove that a hybrid isolation system may be used to further reduce the structural responses, providing better protection to the structure and its contents. These results show that the hybrid isolation system significantly reduces the structural responses, drifts, base shears, and the energy in the structure. The performance of the hybrid system is superior to that of the passive isolation, but this superiority comes at the price of having a much more complicated system, and needing significant energy for the control.

Properly designed nonlinear control algorithms can be used to effectively control the hybrid control system. When these algorithms are property designed, they can accommodate the implementation problems and will work properly in the presence of errors and uncertainties. The results prove that many of the implementation issues may be overcome with well designed controllers and current technology, moreover, the control algorithms that produce these results can be used with a variety of active and hybrid control devices.

Acknowledgements

Funding for this research was provided through the National Center for Earthquake Engineering Research Contracts no. 945101 and 955101, which were supported by the National Science Foundation Master Contract no. BCS 90-25010 and NYSSTF Grant no. NEC-91029

References

1 Brogan, W. L. *Modern control theory*, Prentice Hall, Englewood Cliffs, New Jersey, 1991
2 La Salle, J. and Lefschetz, S. *Stability of Nonlinear Control Systems*, Academic Press, New York, 1961
3 Riley, M. A. 'Experimental implementation and design of a hybrid control system with actuator–structure interaction' Ph.D. Dissertation, Department of Civil Engineering, State University of New York, Buffalo, NY, 1996
4 Dyke, S. J., Spencer, B. F., Quast, P. and Sain, M. K. 'Role of control–structure interaction in protective system design', *J. Engng Mech. ASCE* 1995, **121** (2), 322–338
5 Reinhorn, A. M., Nagarajaiah, S., Subramaniam, R. and Riley, M. A. 'Study of hybrid control for structural and nonstructural systems', *Int. Workshop Struct. Control*, Honolulu, Hawaii, 1993, pp. 405–416
6 Riley, M. A., Subramaniam, R., Nagarajaiah, S. and Reinhorn, A. M. 'Hybrid control of sliding base isolated structures', *Seismic isolation, passive energy dissipation and active control*, vol. 2, Applied Technology Council, Redwood City, CA, 1993. ATC 17-1, pp. 799–810
7 Subramaniam, R. S., Reinhorn, A. M., Nagarajaiah, S. and Riley, M. A. 'Hybrid control of structures using fuzzy logic', *Microcomputers Civil Engng: Special Issue on Fuzzy Logic in Civil Engng* 1996, **11** (1), 1–17
8 Nagarajaiah, S., Riley, M. A. and Reinhorn, A. M. 'Hybrid control of sliding isolated bridges', *J Engng Mech., ASCE* 1993, **119** (11), 2317–2332
9 Reinhorn, A. M., Nagarajaiah, S., Riley, M. A. and Subramaniam, R. 'Hybrid control of sliding isolated structures', *Struct. Engng Natural Hazards Mitigation*, Ang and Vilaverde (eds) 1993, **1**, 766–771
10 Subramaniam, R. S. 'Control of structures using algorithms based on fuzzy set theory', Ph.D. Dissertation, Department of Civil Engineering, State University of New York, Buffalo, NY, 1994
11 Yang, J. N., Li, Z., Danielians, A. and Liu, S. C. 'Aseismic hybrid control of nonlinear and hysteretic structures I', *J. Engng Mech., ASCE* 1992, **118** (7), 1423–1440
12 Yang, J. N., Wu, J. C., Reinhorn, A. M. and Riley, M. A. 'Control of sliding-isolated building using sliding mode control', *J. Struct. Engng. ASCE* 1996, **122** (2), 179–186
13 Riley, M. A., Nagarajaiah, S. and Reinhorn, A. M. 'Hybrid isolation systems for sensitive equipment and secondary systems', *1993 Nat. Earthq. Conf.*, vol. 2, Memphis, Tennessee, 1993, pp. 327–336
14 Yang, J. N., Li, Z. and Vongchavalitkul, S. 'Nonlinear control of buildings using hybrid systems', *Seismic Isolation, Passive Energy Dissipation and Active Control*, vol. 2, Applied Technology Council, San Francisco, CA; 1993, ATC 17–1, pp. 811–822
15 Constantinou, M. C., Mokha, A. S. and Reinhorn, A. M. 'Teflon bearings in base isolation. II: modeling', *J. Struct. Engng. ASCE* 1990, **116** (2), 455–474
16 Yang, J. N., Li, Z. and Liu, S. C. 'Control of hysteretic system using velocity and acceleration feedbacks', *J. Engng Mech., ASCE* 1992, **118** (11), 2227–2245
17 Haas, V. B. 'Coulomb friction in feedback control systems', *Trans. AIEE Applications and Industry*, Part II, **72**, 119–126
18 Truxal, J. G. *Automatic feedback control system synthesis*, McGraw-Hill, New York, 1955
19 Soong, T. T., Reinhorn, A. M. and Yang, J. N. 'A standardized model for structural control and some experimental results', *Structural Control: Proc. 2nd Int. Symp. Struct. Control*, Leipholz, H. H. E. (ed.), Martinus Nijhoff, Boston, pp. 669–693
20 Uang, C-M. and Bertero, V. 'Use of energy as a design criterion in earthquake-resistant design', UCB/EERC-88/18, Earthquake Engineering Research Center, University of California, Berkeley, CA, 1988